Chinese Journal of
POLYMER SCIENCE

RESEARCH ARTICLE

https://doi.org/10.1007/s10118-026-3792-5
Chinese J. Polym. Sci.

Generation and Modulation of Apparent All-angle Dependent Nonreciprocal Chiroptical Response in Chiral Polyurethane Film

Run Zhang, Biao Zhao*, and Jian-Ping Deng*

State Key Laboratory of Chemical Resource Engineering, College of Materials Science and Engineering, Beijing University of Chemical Technology, Beijing 100029, China

Electronic Supplementary Information

Abstract Nonreciprocal chiroptical response, a phenomenon arising from light-matter interaction by the coupling of linear optical effects, attracts rapidly increasing attention to advance fundamental chiroptical theory and develop high-performance optical devices. Herein, we fabricated a chiral polyurethane system with tunable apparent all-angle nonreciprocal chiroptical response, where can be further controlled by modulating the content of doped small molecules within the polyurethane film. Building on these observations, we investigated the origins of the angle-dependence and nonreciprocal chiroptical responses, and proposed a plausible mechanism to explain the emergence of this apparent circular dichroism (CD) signal. Furthermore, we utilized achiral helical polyacetylene to regulate the response wavelength. Our research establishes a clear relationship between polyurethane structure and apparent all-angle nonreciprocal chiroptical response, providing new insights into the connection between chiral materials and linear optical materials.

Keywords Chirality; Linear dichroism; Linear birefringence; Nonreciprocal chiroptical response; Polyurethane

Citation: Zhang, R.; Zhao, B.; Deng, J. P. Generation and modulation of apparent all-angle dependent nonreciprocal chiroptical response in chiral polyurethane film. *Chinese J. Polym. Sci.* https://doi.org/10.1007/s10118-026-3792-5

INTRODUCTION

Chiral materials have great potential in the realm of circularly polarized luminescence materials,[1–3] asymmetric catalysis,[4–6] chiral separation,[7–9] anti-counterfeiting,[10–12] and so on. Chiral substances can normally be categorized into configurational chirality,[13–15] conformational chirality,[16–18] and supramolecular chirality[19–21] based on their structural characteristics. These distinct chiral architectures were characterized using circular dichroism (CD) spectroscopy. Although CD spectroscopy has been widely used for chiral structure characterization, artifacts can become a hidden problem during CD measurements in solid samples. Artifacts arising from linear dichroism (LD) and linear birefringence (LB) are typically regarded as experimental errors because they are not true CD responses. In recent years, the nonreciprocal chiroptical response has gradually emerged as a prominent research focus in chiroptical studies, with further research on solid chiral films. The nonreciprocal chiroptical response refers to the phenomenon in which CD or CPL signals differ when the film is reversed. Such a phenomenon can be realized not only by proper structural design,[22] but also by anisotropic optical responses. The LDLB, characterized by the coupling of LD and LB, is one of the most well-known anisotropic optical responses for the development of nonreciprocal chiroptical systems.[23,24] Specifically, to achieve LDLB, the system must possess both LD and LB, with a non-zero angle between them. Under these conditions, the LD and LB couple to form the LDLB response. Investigating such nonreciprocal chiroptical properties not only deepens the understanding of linear optical materials but also offers unprecedented opportunities in the field of CPL. On the one hand, nonreciprocal materials hold promise for further enhancing the polarization degree in CPL devices.[25] However, nonreciprocal materials offer unprecedented advantages for switchable circularly polarized phosphorescence systems. For example, by constructing nonreciprocal phosphorescent architectures, the polarization direction of circularly polarized phosphorescence can be altered simply by flipping the sample orientation, thereby avoiding structural damage typically associated with complex external manipulation processes. Moreover, nonreciprocal chiroptical response materials also have immense application value in the fields of information transmission and anti-counterfeiting. The feature of achieving signal inversion simply by switching between the front and back sides provides a convenient approach for realizing chiral logic gates. Meanwhile, the expression of distinct chiral information on the front and back sides is expected to become a new dimension of anti-counterfeiting.

Current approaches for decoupling LD and LB predominantly rely on analytical derivations based on Mueller calcu-

* Corresponding authors, E-mail: zhaobiao@mail.buct.edu.cn (B.Z.)
E-mail: dengjp@mail.buct.edu.cn (J.P.D.)
Received May 21, 2026; Accepted June 20, 2026; Published online September 10, 2026

lus. In isotropic systems, the derived formula is:[26]

$$CD_{apparent} = CD_{iso} + 1/2(LD \cdot LB' + LB \cdot LD') + (LD \cdot \sin\alpha + LB) \cdot \cos 2\theta \quad (1)$$

herein, $CD_{apparent}$ represents the experimentally measured CD signal, in which the CD term corresponds to the genuine CD signal arising from intrinsic chiral structures. 1/2(LD·LB'+LB·LD') accounts for the contribution derived from the sample's inherent linear dichroism and linear birefringence (LDLB) effects, while (LD·sinα+LB)·cos2θ originates from optical artifacts induced by the interaction between the sample and the instrument during measurement, where θ describes the sample rotation around the optical axis and α is related to the residual birefringence of the photoelastic modulator. This theory has been successfully applied in LDLB studies on transparent and uniform inorganic and organic crystals. Tempelaar *et al*. made significant contributions to the theoretical framework of nonreciprocal chiroptical responses. In 2021, they proposed a physical mechanism for the generation of nonreciprocal chiroptical responses and experimentally validated it using polythiophene thin films.[27] In 2025, they further advanced the theoretical framework by investigating the origin of nonreciprocal chiroptical responses in centrosymmetric $Li_2Co_3(SeO_3)_4$ crystals.[28] Their work refined the fundamental understanding of nonreciprocal chiroptical responses. In addition to inorganic crystal systems, nonreciprocal chiroptical responses can also be achieved in organic materials through the construction of ordered structures. Di Bari, Albano, and their coworkers made substantial contributions to the field of nonreciprocal chiroptical responses.[25,26] They conducted detailed studies on the step-terrace structures formed in oligothiophene systems after annealing and elucidated the critical role of these structures in generating nonreciprocal chiroptical signals in the samples.

Although crystals with nonreciprocal chiroptical responses have received considerable attention, their practical deployment is severely hindered by their intrinsic brittleness, poor scalability for large-area film fabrication, and incompatibility with flexible substrates. Polymer systems have emerged as superior candidates for next-generation flexible chiroptronics owing to their excellent processability, mechanical robustness, and solution-based manufacturability. Ye and Liu successfully integrated silver nanowires and tempo-oxidized cellulose nanofibers into a waterborne polyurethane matrix.[29] By twisting the composite sample and utilizing its self-healing properties, they achieved distinct CD signals at different angles.

Theoretically, from the perspective of mechanistic research, the inherent multiple scattering, depolarization, and interface effects within polymer systems make the transport paths of photons in a highly complex medium. This indicates that the LDLB coupling mechanism described by the classical formulas can be further modulated by microscopic scattering processes in polymer systems. Therefore, to guide the design of nonreciprocal chirality in polymers while focusing on LD, LB, and their coupling, it is even more necessary to examine how to regulate this macroscopic anisotropic response, which is dominated by scattering and interfaces, through processing strategies. Hong *et al*. investigated the influence of stirring on nonreciprocal CD and CPL responses in a polyethylene naphthalate (PEN) system.[30] They found that the stirring direction, stirring rate, and film thickness after stirring significantly affected the nonreciprocal CD absorption and CPL emission. They attributed this phenomenon to three key factors: sufficient charge transfer (CT) effects at the dopant-polymer interface that govern linear dichroism (LD), rapid-quench-fixed polymer orientation that enables linear birefringence (LB), and vortex-induced chain alignment. Their research demonstrated that the processing method had a significant impact on the formation of nonreciprocal chiroptical responses.

Polymers have become essential components of chiroptical materials.[31,32] On the one hand, the excellent film-forming properties and flexibility of polymers make them ideal matrices for chiral materials, providing a suitable class of materials for chiral separation.[33,34] On the other hand, the unique conformational chirality of chiral polymers enables unique functions, such as chiral amplification and dynamic smart responses.[35] As a widely studied and industrially produced material, polyurethane (PU) exhibits excellent mechanical properties and high design flexibility. Importantly, the PU structure contained hard segments that aggregated into ordered domains. These domains possess well-aligned molecular arrangements that can promote both LD and LB. Consequently, incorporating the nonreciprocal chiroptical response into polyurethane to develop advanced PU-based materials represents a highly promising design strategy. Our research group has successfully demonstrated nonreciprocal chiroptical responses in polyurethane systems through a series of methodologies, including mechanical stretching,[36] electrospinning,[37] and solution casting film formation.[38]

Considering that circularly polarized light interacts with both chiral matter and nonreciprocal chiroptical materials, the nonreciprocal chiroptical response of chiral polyurethane systems remains an untapped area of investigation. Based on these considerations, we introduced polyethylene glycol (PEG) as the soft segment, methylene diphenyl diisocyanate (MDI) as the hard segment, and ethylene glycol and chiral substance (*S*)-(-)-1,1'-bi-2-naphthol as chain extenders and fabricated chiral PU, denoted as BPU. The BPU exhibited an apparent nonreciprocal chiroptical response. Furthermore, the intensity and direction of the apparent nonreciprocal chiroptical response could be changed for each 45° rotation. The influence of thickness, film-forming conditions, and small-molecule doping on the nonreciprocal chiroptical response has been systematically explored, and we found that the origin of the apparent nonreciprocal chiroptical response can be attributed primarily to small-molecule doping-induced assembly. To further validate this mechanism, we removed small molecules from the system and subsequently reintroduced them, achieving precise control over the emergence and disappearance of the nonreciprocal chiroptical response, as illustrated in Scheme 1. Notably, we found that excess small molecules were not limited to MDI, thereby expanding the scope of applicable nonreciprocal systems. It was further found that the film thickness, film-forming conditions, and small-molecule doping can control the apparent nonreciprocal chiroptical response by modulating the microscopic orientation of the structure of the material. In addition, the scattering mechanism within the BPU matrix gives rise to angle-dependent CD signals. Furthermore, we examined the role of

achiral helical-substituted polyacetylene in the nonreciprocal chiroptical response. This work achieved the generation and regulation of the nonreciprocal chiroptical response through a small-molecule doping strategy, providing a universal method for the preparation of polyurethane materials with nonreciprocal chiroptical responses. This study elucidates the fundamental mechanisms underlying the nonreciprocal chiroptical response in polyurethane systems, providing a foundation for future research and application of nonreciprocal chiroptical materials.

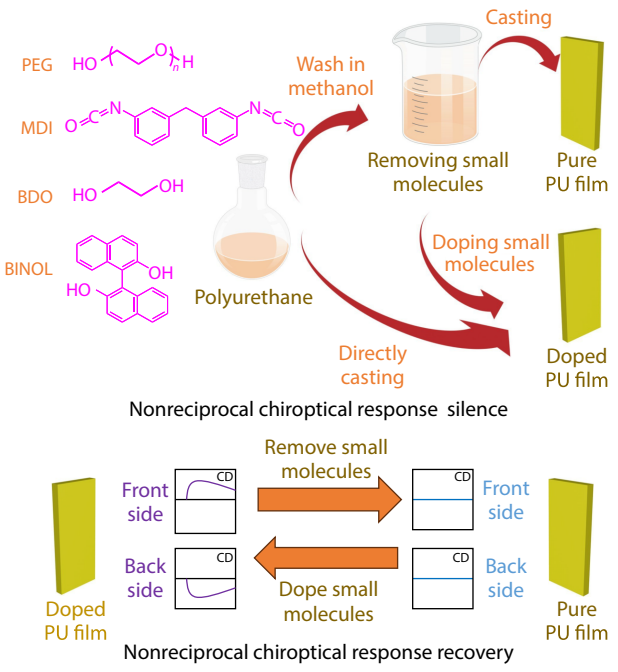

Scheme 1 Synthesis route of BPU film and control of nonreciprocal chirality through adjusting the small molecules.

EXPERIMENTAL

General Considerations

The chiral acetylenic monomer Y[39] was synthesized according to the method described in our previous work. The (nbd)$Rh^+B^-(C_6H_5)_4$ catalyst was prepared according to a previous report.[40] 1,4-Butanediol (BDO), dibutyltin dilaurate (DBTDL) and PEG2000, were obtained from J&K. (*S*)-1,1'-Bi-2,2'-naphthol (S-BINOL) and MDI were purchased from Macklin. Benzoquinone (Bq) was purchased from Chemical Reagent Co. Resorcinol was purchased from Innochem (Shanghai, China). All commercially available chemicals were used as received. The polymer films were identified using Fourier-transform infrared spectroscopy (FTIR, Bruker Tensor II). The CD and UV-Vis absorption spectra were obtained using a Jasco-810 spectropolarimeter. Scanning electron microscopy (SEM) was performed using a FlexSEM 1000 II instrument.

Preparation of Helical Polymers

PY was synthesized according to previously described methods.[39,40] Achiral monomer Y (52 mg, 0.3 mmol) and (nbd)$Rh^+B^-(C_6H_5)_4$ (1 mol% of monomer) were dissolved in 3 mL of $CHCl_3$, and the polymerization was performed in a N_2 atmosphere at 30 °C for 4 h. The resulting solution was poured into a large quantity of *n*-hexane to precipitate the polymer. The precipitate was filtered and dried under vacuum at 25 °C for 12 h, yielding solid PY (yield: 96%). The other helical polymers were prepared in the same manner.

Preparation of BPU Film

Add 1 g of PEG2000 into a 100 mL single necked flask, and 30 mL of dichloromethane/tetrahydrofuran was added for complete dissolution. MDI (300 mg of MDI with a small amount of dichloromethane, added to a single-necked flask, mixed well, and 5 μL of DBTDL was added. The flask was placed in a water bath at 40 °C and magnetically stirred for 2 h. Subsequently, 0.045 g of BDO and 14.32 mg of BINOL were added to the reaction mixture and the reaction was allowed to proceed for an additional 2 h. After the reaction, the solvent was removed by rotary evaporation, and the product was injected into a tetrafluoroethylene mold with a 1 mL syringe and cured in an air drying oven at 45 °C for 8 h to obtain the PU film.

Preparation of Purified BPU Film and Re-doped BPU Film

The synthetic steps were consistent with those described in the **Preparation of BPU Film** section. After the reaction, the system was diluted with an appropriate amount of THF and poured into 300 mL of methanol to form a suspension. The suspension was then transferred to centrifuge tubes and centrifuged at 1×10^4 r/min for 3 min. The solid precipitate was collected, redissolved in 3 mL of THF, and cast into a film to obtain the purified BPU film. After adding 3 mL of THF to the re-doped BPU film, a specific amount of Bq/Res/PY was introduced. Once the solid was fully dissolved, the solution was cast into a film to yield a redoped BPU film.

Molecular Dynamics (MD) Simulation Details Model Construction

Consider the BPU and BPU-Bq systems as examples. Amorphous models of the BPU and BPU-Bq systems were constructed using the Amorphous Cell module in Materials Studio. In the BPU system, three polymer chains consisting of PEG soft segments and chiral hard segments (MDI and binaphthol units) were included. For the BPU/Bq system, 17 Bq molecules were randomly dispersed in a BPU matrix to investigate the doping effect. The initial cells were constructed with a low density of 0.3 g/cm^3 to avoid atom overlapping.

Forcefield and Parameters

All the simulations were performed using the COMPASS III force field, which was optimized for condensed-phase organic polymers. Atomic charges were assigned based on forcefield-assigned values. The Ewald summation method was used for electrostatic interactions and an atom-based method with a cut-off distance of 12.5 Å was applied for van der Waals interactions.

Simulation Procedures

A multi-step equilibration protocol was implemented to obtain realistic microstructures, each of which underwent rigorous energy minimization using the Smart algorithm (fine quality) to eliminate the initial strain. To induce microphase separation and escape the local energy minima, a simulated annealing process was performed in the NPT ensemble (10^{-4} GPa). The temperature was cycled between 300 and 600 K for five cycles, with each cycle consisting of 20 heating/cooling ramps. The final density

stabilized at approximately 1.1 g/cm^3, consistent with the experimental values. Following annealing, a Production Dynamics run was performed in the NVT ensemble at 298 K for 500 ps (with a time step of 1.0 fs) to collect the trajectories for further analysis.

Data Analysis

The radial distribution function (RDF) was analyzed to evaluate the self-aggregation of the hard segments and the influence of Bq.

RESULTS AND DISCUSSION

Apparent Angle-dependent Nonreciprocal CD Response

BPU was synthesized for further experiments. Specifically, poly(ethylene glycol) (PEG) and methylene diphenyl diisocyanate (MDI) functioned as the soft and hard segments in the PU chains, while 1,4-butanediol (BDO) and chiral 1,1'-bi-2,2'-naphthol (BINOL) were used as chain extenders, in which S-BINOL was chosen as a representative for research. Herein, excess MDI was used to ensure the complete reaction of the hydroxyl groups. All the synthesis routes are presented in the **EXPERIMENTAL** section. Attenuated total reflectance Fourier transform infrared spectroscopy (ATR-FTIR) was used to illustrate the generation of BPU. As shown in Fig. S1 (in the electronic supplementary information, ESI), the characteristic peaks assigned to the C=O stretching vibration and N—H bending vibration of the urethane groups appeared at 1725 and 1533 cm^{-1}, respectively. Simultaneously, the characteristic absorption peak of the —NCO group of the MDI monomer at approximately 2270 cm^{-1} completely disappeared, indicating the complete reaction of the isocyanate groups. In addition, the typical C—O—C ether bond stretching vibration band of the PEG soft segment was retained at 1090 cm^{-1}, while the vibration peaks attributed to the naphthalene ring skeleton and C—H out-of-plane bending of BINOL were observed at 1599, 1509, and 816 cm^{-1}. The aforementioned 'formation of new bonds' and 'retention of characteristic monomer skeletons' fully demonstrate the successful preparation of the BPU. GPC analysis further confirmed the successful polymerization of BPU with a molecular weight of 1.5×10^4 level. Therefore, it was concluded that the BPU was successfully obtained.

The CD spectrum was measured to illustrate the chirality of BPU-CH_2Cl_2, the solvent is CH_2Cl_2 in the film-forming process. The measurements were performed by flipping the film and rotating it along its optical axis. Specifically, the side exposed to air during preparation was defined as the front side, whereas the side in contact with the mold was designated as the back side. The rotational method is illustrated in Scheme S1 (in ESI). Specifically, when the front side of the sample faced the light source, it was rotated counterclockwise around the optical axis; when the back side faced the light source, it was rotated clockwise around the optical axis. As shown in Figs. 1(a) and 1(d), on the front side, BPU-CH_2Cl_2 exhibits a CD signal at 370 nm, which is positive at 0° (180°) and 135° (315°) and negative at 45° (225°) and 90° (270°). However, the signals at all the angles were reversed on the back side. Positive CD signals were observed at 45° (225°) and 90° (270°), while negative CD signals were observed at 0° (180°) and 135° (315°). The peak wavelength remained constant at 370 nm. These phenomena indicate that the BPU-CH_2Cl_2 film exhibited an apparent angle-dependent nonreciprocal chiroptical response at all angles.

Furthermore, the chiroptical activity inherent to the BPU structure became undetectable upon film formation. This phenomenon is primarily ascribed to light scattering effects, which lead to the distortion of BPU's intrinsic chiral signals of the BPU. Consequently, we term this observation "apparent nonreciprocal chiroptical response," emphasizing that it originates from the superposition of scattering on molecular chirality. A more detailed discussion of this mechanism will be provided in the subsequent **Effects of Scattering on the Nonreciprocal Chiroptical Response** section.

Effects of Film-forming Solvents and Film Thickness

Because the interaction between the film and light is significantly affected by the optical path length, which is directly related to the film thickness, we investigated the effect of the film thickness on the apparent angle-dependent nonreciprocal chiroptical response of the BPU. The film thickness was controlled by adjusting the concentration of the film-forming solution. Thickness characterization was performed using a thickness gauge by averaging measurements taken at three random locations on the film surface. The thick BPU films, taking BPU-CH_2Cl_2 as an example, measured 100–200 μm in thickness, while the thin BPU films ranged between 30 and 60 μm. Compared to the thick BPU film explored above, the thin BPU film, denoted as BPU-Thin, exhibited intrinsic chirality affected by the apparent angle-dependent nonreciprocal chiroptical response, as shown in Figs. 1(b) and 1(e). Specifically, BPU-Thin exhibited a negative CD signal at 320 nm stemming from its intrinsic chirality. At 365 nm, the CD signal shows an angle-dependent nonreciprocal chiroptical response consistent with thicker films, where positive CD signals appear at 0° (180°) and 135° (315°), whereas negative signals occur at 45° (225°) and 90° (270°). This phenomenon illustrates that a thicker film can generate a stronger apparent angle-dependent nonreciprocal chiroptical response. To further confirm the intrinsic chirality of the BPU, we characterized the corresponding BPU solution before casting. As Fig. S2 (in ESI) shows that the BPU solution exhibited a negative CD signal at 307 nm, which corresponds to BPU-Thin. The above findings illustrate that the expressions of nonreciprocal chirality and intrinsic chirality are affected by the film thickness. This phenomenon is attributed to scattering, as discussed in detail in **Molecular Dynamics (MD) Simulation Details Model Construction** section. Because the intrinsic chirality of BPU films has been thoroughly characterized, subsequent experiments were focused exclusively on thick films (100–200 μm) to more clearly observe the emergence and evolution of the apparent angle-dependent nonreciprocal chiroptical response.

To further explore the relationship between the apparent angle-dependent nonreciprocal chiroptical response and BPU films, we investigated the effect of different solvent evaporation processes on the apparent CD spectra of BPU films. While CH_2Cl_2 was used as the reaction solvent in the above experiments, we further prepared BPU-THF films using THF as the film-forming solvent to examine solvent effects. The BPU-THF films displayed enhanced apparent angle-dependent non-reciprocal chiroptical signals. The front side showed positive CD

https://doi.org/10.1007/s10118-026-3792-5

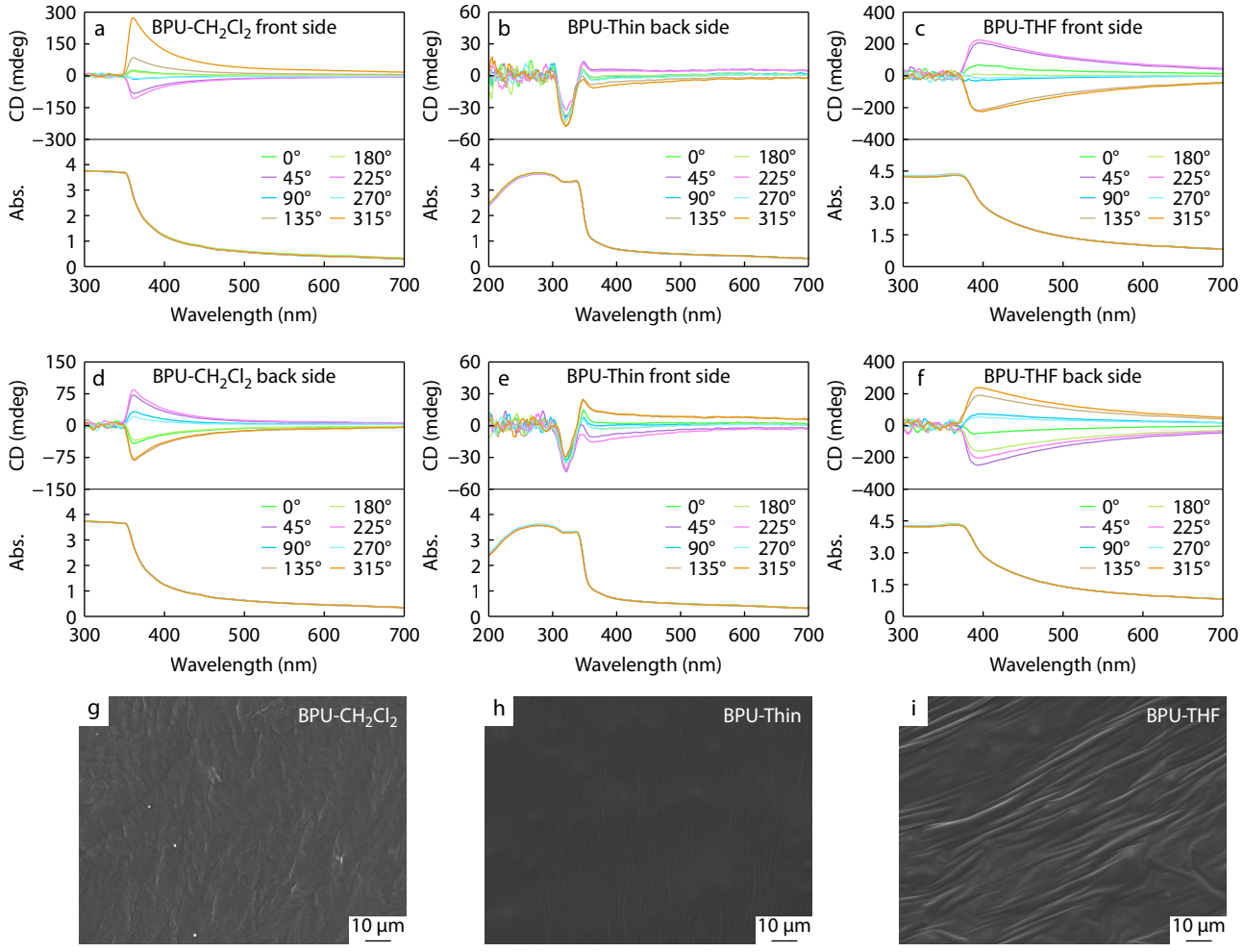

Fig. 1 (a, d, g) are front side, back side, and SEM image of surface structure of BPU film; (b, e, h) are front side, back side, and SEM image of surface structure of BPU thin film; (c, f, i) are front side, back side, and SEM image of surface structure of BPU-THF film.

signals at 0° (180°) and 45° (225°), and negative CD signals at 90° (270°) and 135° (315°), while the back side exhibited the opposite pattern, with positive signals at 90° (270°) and 135° (315°), and negative signals at 0° (180°) and 45° (225°), demonstrating an all-angle nonreciprocal chiroptical response. By comparing the characterization results of the BPU-CH_2Cl_2 and BPU-THF films, it is evident that film-forming processes controlled by different solvents lead to distinct CD signals. Specifically, the differences manifest in the angle-dependent patterns, intensity of the CD signals, and wavelengths of the apparent angle-dependent nonreciprocal chiroptical response. When THF was employed as the casting solvent, the results obtained at each angle were opposite to those of the BPU-CH_2Cl_2 film, and the CD signal intensity was significantly higher. For instance, when measured at an angle of 45° on the front side, the BPU-CH_2Cl_2 film exhibited a negative CD signal, whereas the BPU-THF film exhibited a positive signal. Furthermore, the absolute CD value of the BPU-THF film in this orientation was approximately 200 mdeg, which is markedly higher than that of the BPU-CH_2Cl_2 film (120 mdeg). In addition, a comparison of Figs. 1(a), 1(d), 1(c) and 1(f) reveals a distinct redshift in the CD peak position of the BPU-THF film relative to that of the BPU-CH_2Cl_2 film. These experimental results indicate that the angle-dependent nonreciprocal chiroptical response is directly correlated with the film formation process. Considering the boiling points of THF and CH_2Cl_2, it seems that a relatively lower film-forming rate promotes the development of stronger CD signals and influences the specific manifestations of the angle dependence.

Among the BPU-CH_2Cl_2, BPU-THF, and BPU-Thin samples mentioned above, there was a noticeable variation in the strength and responsive wavelength of the nonreciprocal CD response. To further investigate the reasons behind these changes in the nonreciprocal chiroptical responses, we characterized the surface scanning electron microscopy (SEM) of the three sample systems. As shown in Fig. 1(g), the BPU-CH_2Cl_2 surface exhibits a certain orientation, indicating the presence of LD and LB effects in the system. The effect of LD was also observed in the BINOL group. Although oriented structures simultaneously generate both LD and LB, there is typically no angular offset between them, thereby preventing the realization of nonreciprocal chiroptical responses. However, in Fig. 1(h), the oriented structure of BPU-Thin became less distinct, accompanied by a significant reduction in the nonreciprocal chiroptical response. In Fig. 1(i), the oriented structure is more pronounced than in Fig. 1(g), and the

https://doi.org/10.1007/s10118-026-3792-5

nonreciprocal chiroptical response also shows a marked increase. In summary, the orientation structure and nonreciprocal chiroptical response exhibited a clear positive correlation. As the orientation strengthens in the BPU film, the nonreciprocal chiroptical response also demonstrates significant enhancement. This indicates that an oriented structure is one of the conditions for generating a nonreciprocal chiroptical response.

Effects of Doped Small Molecules

In previous studies,[38] we proposed that excess small molecules in the system promote the formation of non-reciprocal CD signals. To verify this hypothesis, we removed excess small molecules (MDI) and examined the resulting changes in the chiroptical properties of the as-purified film. A detailed procedure for the removal of small molecules is provided in the **EXPERIMENTAL** section. CD measurements of the purified BPU films are shown in Figs. S3(a) and S3(b) (in ESI) showing no detectable signals for either intrinsic chirality or nonreciprocal chiroptical responses. This phenomenon had two key aspects. First, the disappearance of intrinsic chirality in BPU-purified films is not due to the masking of chiroptical signals by the nonreciprocal chiroptical response, because no nonreciprocal chiroptical response was observed in the purified BPU films. In contrast, the angle-dependent nonreciprocal chiroptical response was significantly correlated with the doping of small molecules. To further investigate the role of excess small molecules in the formation of a nonreciprocal chiroptical response, we introduced benzoquinone (Bq) into purified BPU to prepare the BPU-Bq film. As shown in Figs. 2(a) and 2(b), the CD spectra of BPU-Bq exhibit a significant nonreciprocal chiroptical response at 368 nm. When the front side of the film was tested, positive CD signals were observed at 0°, 45°, 180°, and 225°, whereas negative CD signals were observed at 90°, 135°, 270°, and 315°. When the backside was tested, the peak position remained unchanged at 368 nm. However, BPU-Bq exhibited positive CD signals at 90°, 135°, 270°, and 315° and negative CD signals at 0°, 45°, 180°, and 225°. These results indicate that the nonreciprocal chiroptical response reappears in the BPU-Bq films after doping with Bq small molecules.

To investigate the effect of the dopant molecular structure and the universality of this method for achieving a nonreciprocal chiroptical response in polyurethane systems, we prepared BPU films doped with resorcinol (Res) small molecules, denoted as BPU-Res. The CD spectra of BPU-Res are shown in Figs. 2(d) and 2(e), with a CD peak located at 360 nm. Similarly, when the front side of the film was tested, positive CD signals were observed at 0°, 45°, 180°, and 225°, whereas negative signals were observed at 90°, 135°, 270°, and 315°. Upon testing the back side, the peak position remained at 360 nm; however, BPU-Res exhibited positive CD signals at 90°, 135°, 270°, and 315° and negative signals at 0°, 45°, 180°, and 225°. These results demonstrate that angle-dependent nonreciprocal chiroptical responses also emerge in the BPU-Res films after the incorporation of Res. The surface morphologies of the two films were characterized by SEM. As shown in Figs. 2(c) and 2(f), both films exhibit pronounced oriented structures on their surfaces, which is consistent with the results previously observed for BPU-CHCl2, BPU-Thin, and BPU-THF. These observations clearly demonstrate that small-molecule doping can facilitate angle-dependent nonreciprocal chiroptical activity within the systems.

To further elucidate the role of small molecules in the for-

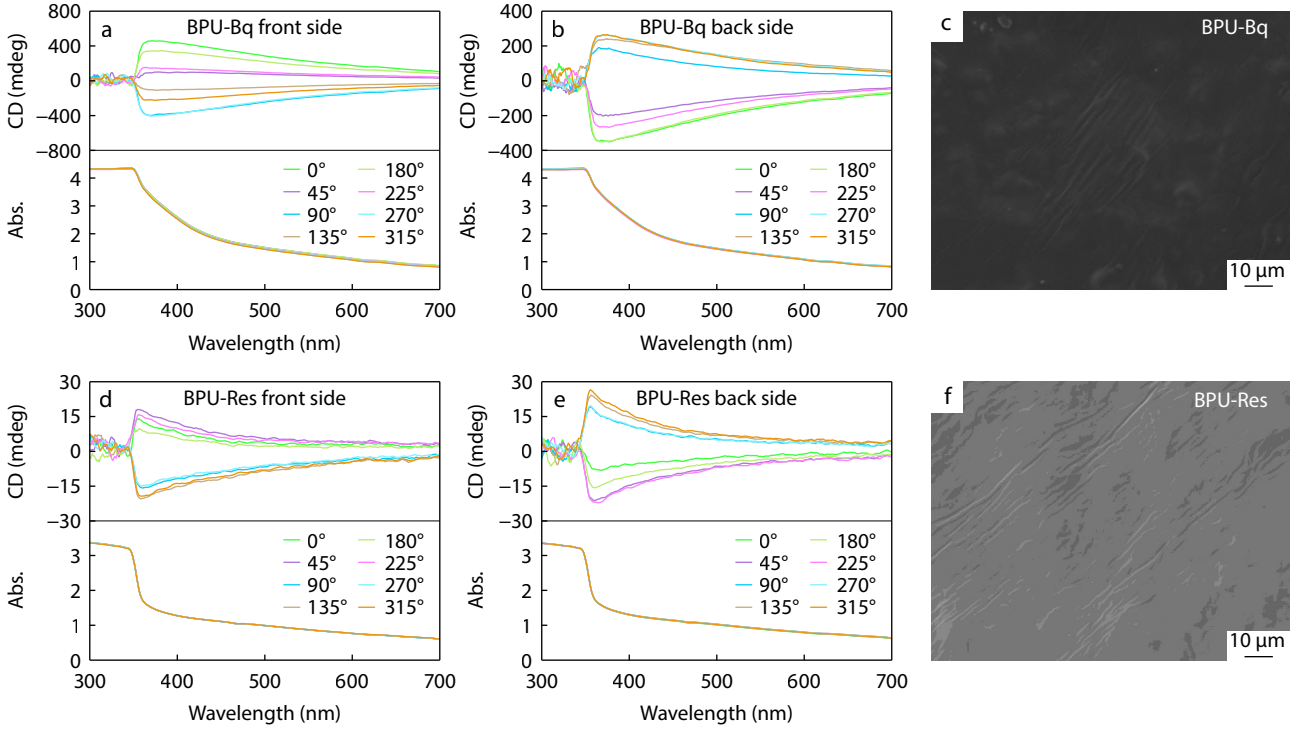

Fig. 2 CD spectra of BPU-Bq in the (a) front side and (b) back side, and (c) SEM image of BPU-Bq; CD spectra of BPU-Res in the (d) front side and (e) back side, and (f) SEM image of BPU-Res.

https://doi.org/10.1007/s10118-026-3792-5

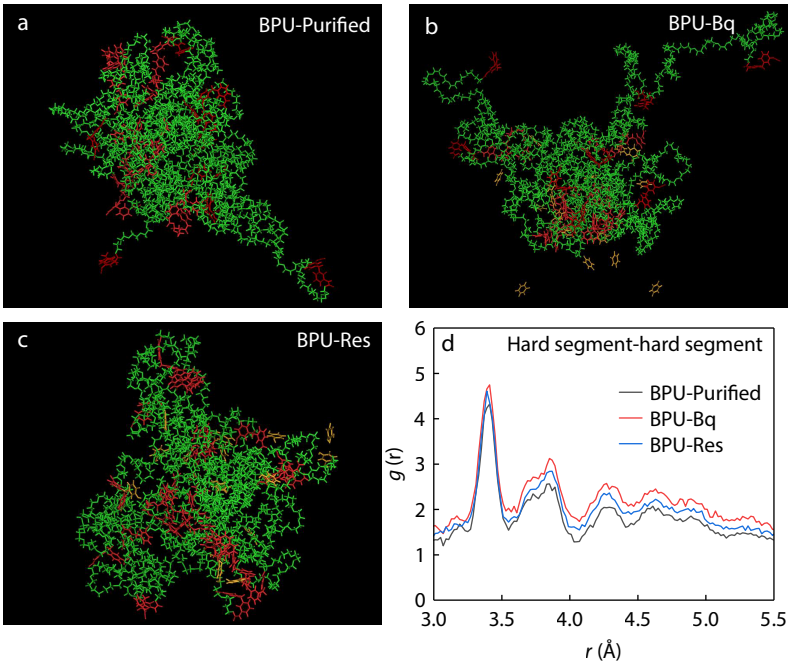

Fig. 3 (a–c) show the molecular dynamic simulation images of BPU-Purified, BPU-Bq, and BPU-Res, respectively. The green, red, and orange parts are the soft segments, hard segments, and doped small molecules, respectively. (d) is the RDF among the hard segments.

mation of the nonreciprocal chiroptical response, computational simulations were performed using Materials Studio 5.5. Detailed computational procedures are provided in ESI. As shown in Figs. 3(a)–3(c), BPU-purified, BPU-Bq, and BPU-Res all exhibit microphase-separated structures. To further analyze the generation of these structures, we calculated the radial distribution function (RDF) between the hard segments of the BPU system. The RDF reflects the deviation in the spatial distribution of specific atom pairs relative to the ideal random distribution. Consequently, it can be utilized to quantitatively evaluate the aggregation behavior of hard segments and the specific impacts of various non-covalent interactions on the microphase separation process.[41,42] The RDF of the hard segments for BPU-Bq and BPU-Res shows significantly higher peak intensities in the 3.8 Å range compared to that of the purified BPU (*i.e.*, without the doped small molecules), as shown in Fig. 3(d). This suggests that the addition of small molecules leads to the formation of more ordered structures within the hard domains of BPU-Bq and BPU-Res by strengthening *π*-*π* stacking. Meanwhile, owing to the presence of conjugated systems in Bq and Res, which absorb light, the ordered structure formed by *π*-*π* stacking can further generate LD and LB. Based on these analyses, we propose that the incorporation of small molecules facilitates the formation of well-ordered structures, which, in turn, promotes the generation of new LD and LB factors within the BPU system. As this microscopic ordered structure is unrelated to the orientation mentioned in **Preparation of Helical Polymers** section, its LD and LB contributions are misaligned with those of the oriented structure. Owing to the different LD/LB ratios of these two structural origins, their combination results in an angular offset between the total LD and total LB, which drives the emergence of LDLB coupling in the BPU film.

Effects of Film Thickness, Solvents, and Small-molecule Doping on the Micro-orientation

To further investigate the factors influencing the structure of BPU films, we initially employed SEM to characterize the cross-sectional oriented structures of the films with varying thicknesses. As shown in Figs. S4(a) and S4(b) (in ESI), a distinct cross-sectional orientation exists in both thick and thin BPU films. However, the cross-sectional orientation structure is more pronounced in thick unpurified BPU films than in thin films, indicating a clear correlation between the orientation of the cross-sectional structure and the thickness of the BPU film. We speculate that this phenomenon most likely contributed to the influence of film thickness on the film-forming duration. As the thickness increased, a longer evaporation duration allowed the BPU molecular chains to align more readily along the evaporation direction. To further validate this conclusion and investigate the effect of the solvent evaporation rate on the structure of BPU films, we compared the cross-sectional orientations of BPU-CH_2Cl_2 and BPU-THF films with identical thicknesses. As shown in Figs. S4(a) and S4(c) (in ESI), CH_2Cl_2 exhibits higher volatility and a shorter film-forming time because of its lower boiling point, resulting in less developed orientation structures compared to BPU-THF films and consequently weaker CD signals. This phenomenon indicates that the solvent evaporation process leads to the formation of orientational structures perpendicular to the film surface, which is consistent with the conclusions of our previous study.[38]

To further elucidate the relationship among doping small molecules, cross-sectional orientation, and nonreciprocal CD response, we characterized the orientation structures in the samples after small-molecule removal. In Fig. S4(d) (in ESI), the residual orientation is faintly visible after MDI removal, which is due to the limited hard domain formation during solvent evaporation; however, the structure is insufficient to

https://doi.org/10.1007/s10118-026-3792-5

generate a significant nonreciprocal chiroptical response and only produces minor signals. In contrast, the samples with re-doped small molecules (Figs. S4e and S4f in ESI) exhibited well-defined orientation structures. These results confirmed that excess small molecules play a critical role in facilitating the formation of oriented cross-sectional structures, which are essential for robust nonreciprocal chiroptical responses. Consequently, small molecules play a dual role in the emergence of nonreciprocal CD responses in BPU by promoting the formation of both macroscopic orientations and microscopically ordered structures. The synergy between these two structural features ultimately drives the observed chiroptical behavior.

Effects of Scattering on the Nonreciprocal Chiroptical Response

In the aforementioned study, we observed that the polyurethane system possesses an inherent microphase-separated structure along with an angle-dependent nonreciprocal chiroptical response. We hypothesized that this microphase separation leads to significant multiple scattering effects within the film. This hypothesis is supported by the fact that the intrinsic chirality signals of the BPU films decreased markedly with increasing thickness (Figs. 1a–1d). Generally, for chiral samples, as the sample thickness increases, the chiroptical signals are enhanced owing to the increased interaction distance between the light and the sample. However, when scattering processes are present in the system, they induce a pronounced depolarization effect, which results in the attenuation of the true chiroptical signals, thereby leading to the weakening of the true chiral signal as the film thickness increases. Furthermore, multiple scattering may be one of the underlying causes for the formation of angle-dependent nonreciprocal CD signals. A study by Kotov *et al.*[43] detailed the origins of LDLB coupling in two-dimensional achiral oriented materials, demonstrating that the angle α' between the LD and LB axes significantly influences the resulting CD signals. In the scattering system formed by the polyurethane microphase-separated structure, the hard domains constitute the ordered structures. Consequently, when light passes through the BPU film, it encounters not only the LD induced by the macroscopic orientation, but also the LB and scattering effects arising from the microphase separation. When these scattering effects are combined with LD and LB, they may facilitate the re-coupling of optical paths, giving rise to new signals.

To verify this hypothesis, we investigated the influence of scattering on the chiroptical properties of BPU films, using BPU-Bq as a representative model. Specifically, BPU-Bq was characterized *via* diffuse transmission circular dichroism (DTCD), employing an integrating sphere to collect all light transmitted through the film. The test results are presented in Figs. S5(a) and S5(b) (in ESI). When the front side of the film faced the light source, BPU-Bq exhibited positive CD signals at all rotational angles, with the signal profiles being almost linear. The significant discrepancy between the CD signals of BPU-Bq in the DTCD test and those from the conventional CD test (Figs. 2a and 2d) indicated the presence of scattering effects within the system. Moreover, straight-line CD signals are characteristic of the LD and LB. Additionally, when the back side of the film faced the light source, BPU-Bq displayed negative DTCD signals at all angles, maintaining a nearly straight line profile. This indicates that BPU-Bq exhibits a nonreciprocal chiroptical response originating from LDLB coupling; however, this response is substantially modulated by scattering effects during the measurement, resulting in a pronounced angle dependence.

As mentioned previously (Figs. 3a and 3b), no intrinsic chirality signal was observed in the BPU-purified film after the removal of the small molecules. This phenomenon can also be explained by the scattering effects. We measured the CD spectra of the BPU-purified film in diffuse transmission circular dichroism (DTCD) mode, and the results are shown in Fig. S6 (in ESI). The BPU-purified film exhibited a negative CD peak at approximately 320 nm. This was consistent with the description in Fig. S2 (in ESI) and originates from the intrinsic chirality of the BPU molecules. Therefore, we speculate that the failure to detect the chirality of the BPU-purified film in conventional CD measurements is due to depolarization and polarization scrambling effects caused by the scattering elements within the film, which ultimately leads to the disappearance of the true chiral signal.

In this context, the multiple scattering induced by microphase separation does not merely play a negative role through depolarization; instead, it acts as an "optical path amplifier," significantly enhancing the nonreciprocal signals generated by the coupling of LD and LB. However, it is worth noting that the CD signals resulting from the synergy between scattering and the LDLB should theoretically be randomly distributed between 0° and 180° without a discernable and definite pattern. Given that scattering is dependent on both the incident wavelength and particle dimensions, and considering that significant scattering is primarily observed in the shorter wavelength region, we hypothesize that the scattering originates from ordered structures, specifically hard domains, formed by the accumulation of excess small molecules within the polyurethane matrix. Furthermore, because these hard domains are uniformly distributed throughout the BPU, the scattering process itself is inherently isotropic. Notably, because LDLB signals persist even when an integrating sphere is employed, we propose that the synergy between LDLB coupling and scattering effects fundamentally drives the emergence of this apparent all-angle-dependent nonreciprocal chiroptical response.

The orientation perpendicular to the film surface generated during the film-forming process may also contribute to the all-angle nonreciprocal chiroptical response (Scheme 2). Owing to external perturbations during solvent evaporation, this oriented structure cannot be perfectly perpendicular to the film surface. Consequently, a specific tilt angle exists between the oriented structure and the surface normal, which creates a linear projection onto the plane of the film. This macroscopic projection directly determines the effective LD axis of the film, thereby breaking in-plane optical symmetry. As the sample rotates, the LB effect exhibits a macroscopically isotropic characteristic owing to the scattering mechanism, meaning that it remains invariant during rotation. Therefore, during sample rotation, only the LD axis changed its orientation relative to the LB axis. This leads to a continuous variation in α' between the LD and LB axes, ultimately realizing the observed angle-dependent nonreciprocal signals, as shown in Scheme 3.

https://doi.org/10.1007/s10118-026-3792-5

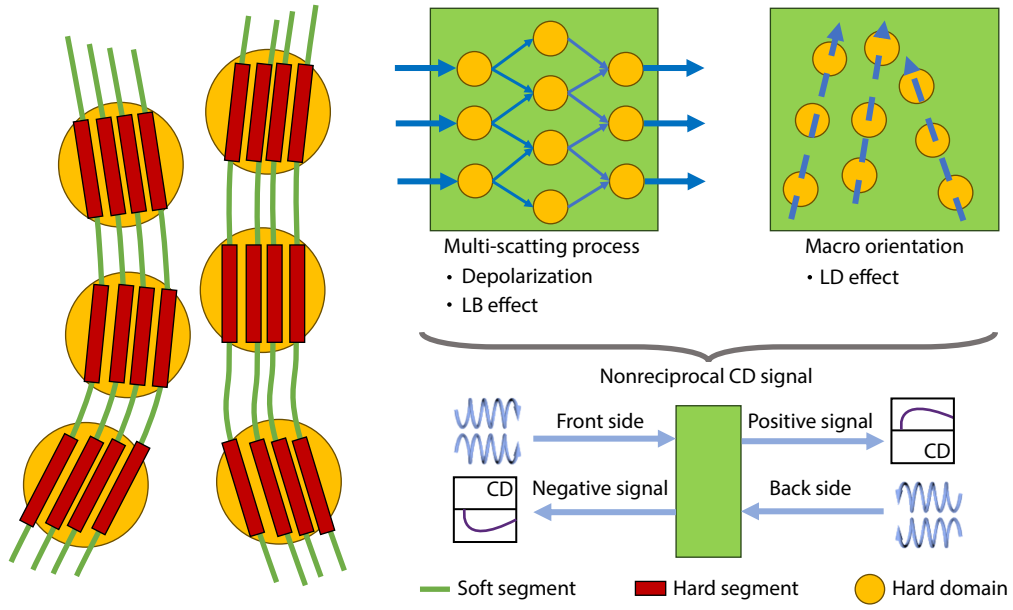

Scheme 2 Microphase separation structure of BPU for generating LD, LB, and nonreciprocal chiroptical response.

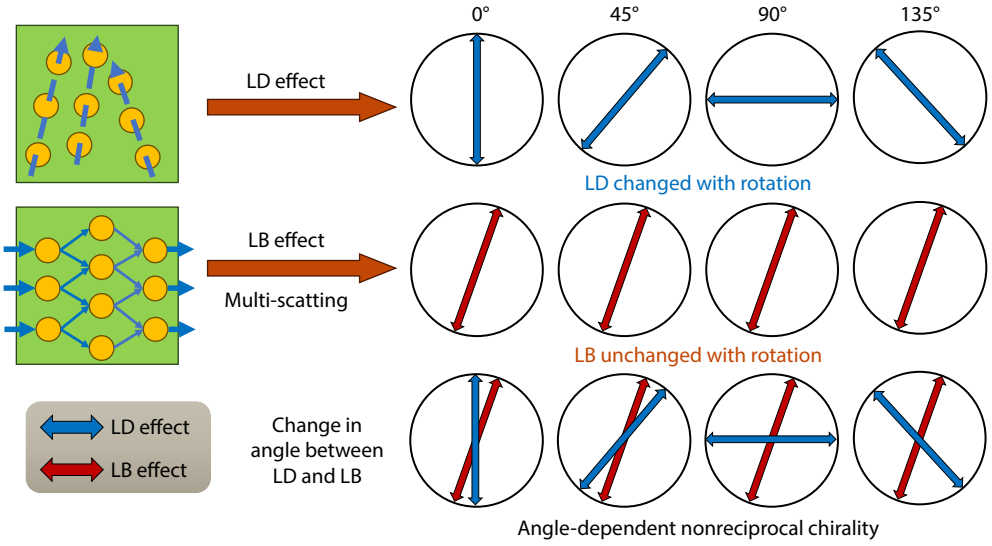

Scheme 3 Possible mechanism of angle-dependent nonreciprocal chiroptical response.

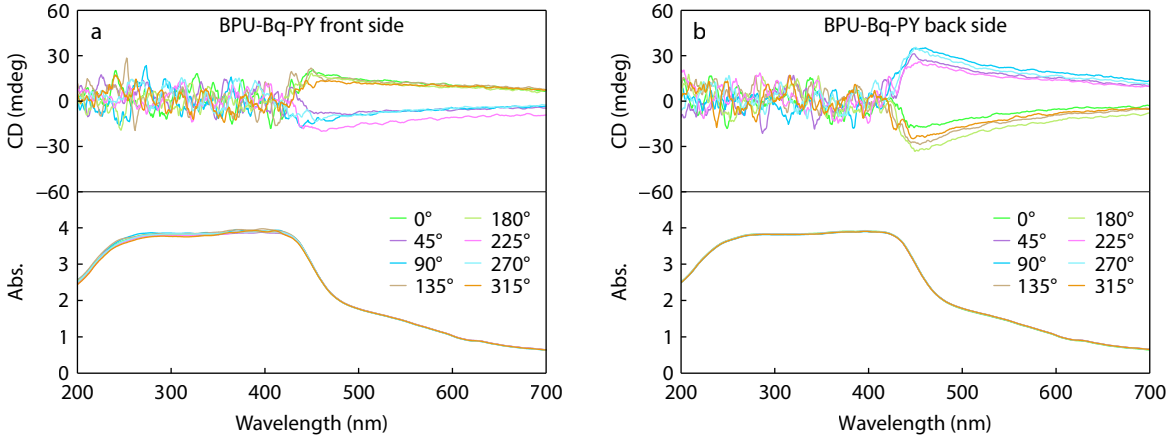

Fig. 4 CD spectra of BPU-Bq-PY in the (a) front side and (b) back side.

https://doi.org/10.1007/s10118-026-3792-5

Modulation of Angle-dependent Nonreciprocal Chiroptical Response with Helical Polyacetylene

In previous studies,[38] we observed that the incorporation of helical-substituted polyacetylene induces a redshift in the angle-dependent nonreciprocal chiroptical response. To further investigate this phenomenon, we introduced helical polyacetylene (PY) into the BPU-Bq system to prepare BPU-Bq-PY and characterized its CD spectrum. As shown in Figs. 4(a) and 4(b), compared to BPU-Bq, BPU-Bq-PY also exhibited all-angle nonreciprocal chiroptical signals with a redshift to 450 nm. This demonstrates that polyacetylene can modulate the generation wavelength of the all-angle non-reciprocal chiroptical response.

We further investigated the role of achiral polyacetylene by directly doping purified BPU with PY to prepare BPU-PY films. The resulting BPU-PY films exhibited no detectable non-reciprocal chiroptical responses, as shown in Fig. S7 (in ESI), indicating that polyacetylene only serves an auxiliary function in modulating the nonreciprocal chiroptical response rather than generating a nonreciprocal chiroptical response. In addition, as shown in Figs. S8(a) and S8(b) (in ESI), SEM imaging revealed a significantly weakened surface orientation in BPU-PY compared to that in BPU-Bq-PY. This demonstrates that the generation of the surface orientation structures shows no direct correlation with helical-substituted polyacetylene but is exclusively governed by the chiral architecture of polyurethane and the doped small molecules. Moreover, the observed changes in the cross-sectional orientation before and after the addition of Bq further substantiate our earlier hypothesis that excess small molecules actively participate in the formation of cross-sectional oriented structures, as shown in Figs. S6(c) and S6(d) (in ESI). The above results indicate that the achiral helical polyacetylene can only modulate the nonreciprocal chiroptical response, rather than directly promoting its generation.

CONCLUSIONS

In conclusion, we reported an apparent all-angle nonreciprocal chiroptical response in BPU systems. The apparent all-angle nonreciprocal chiroptical response is enhanced with an increase in the film thickness and decrease in the film formation rate. To validate the critical role of small molecules in generating an angle-dependent nonreciprocal chiroptical response, we systematically modulated the presence/absence of nonreciprocal chiroptical responses by removing and reintroducing small molecules. We proposed a mechanism based on the co-effect of LD, LB, and the multi-scattering effect for generating the angle-dependent nonreciprocal chiroptical response by molecular dynamic simulation. The angle-dependent nonreciprocal chiroptical response originated from the coupling of the LD contributed by the solvent-induced oriented structure during film formation, LB generated by the ordered stacking structure, and scattering effect from the microphase. Furthermore, the incorporation of helical-substituted polyacetylenes into BPU controlled the wavelength of the nonreciprocal chiroptical response. This study provides insights into the formation mechanism of the all-angle nonreciprocal chiroptical response and advances the fundamental understanding of this interesting phenomenon. It should be mentioned that the nonreciprocal chiroptical responses of polymer materials is a newly emerging research topic. More work is needed to fully understand these effects, which is expected to enable unprecedented chiroptical materials with broad application prospects.

Conflict of Interests

The authors declare no interest conflict.

Electronic Supplementary Information

Electronic supplementary information (ESI) is available free of charge in the online version of this article at http://doi.org/10.1007/s10118-026-3792-5.

Data Availability Statement

The related data (DOI/CSTR: 10.1007/s10118-026-3792-5) for this paper is available in the (Generation and modulation of apparent all-angle dependent nonreciprocal chiroptical response in chiral polyurethane film) database (https://www.scidb.cn/c/cjps).

ACKNOWLEDGMENTS

This work was financially supported by the National Natural Science Foundation of China (No. 52273165) and Fundamental Research Funds for the Central Universities (No. buctrc202225).

REFERENCES

1 Zhao, J. Y.; Shi, S.; Zhang, X. Y.; Liu, D.; Song, F. Y.; Cheng, Y. X.; Li, F. Circularly polarized luminescence pyrene materials: from design to applications. *Coord. Chem. Rev.* **2026**, *548*, 217173.
2 Zhang, D. W.; Li, M.; Chen, C. F. Axially chiral materials exhibiting blue-emissive ultralong organic phosphorescence and intense circularly polarized luminescence. *Sci. China Mater.* **2023**, *66*, 4030−4036.
3 Liu, C.; Zeng, J.; Jiang, Z. H.; Chen, Y. H.; Zhang, J. S.; Cheng, Y. X. A chiral co-assembled exciplex host achieved extremely outstanding narrowband circularly polarized electroluminescence. *Chem. Sci.* **2026**, *17*, 7064−7070.
4 Ji, C.; Zou, X.; Gao, D. Catalytic asymmetric construction of nonadjacent stereoelements. *Angew. Chem. Int. Ed.* **2025**, *64*, e202504224.
5 Jiang, H.; He, X.; Jiang, X.; Zhao, W.; Lu, L.; Cheng, Y.; Xiao, W. Photoinduced Cobalt-catalyzed desymmetrization of dialdehydes to access axial chirality. *J. Am. Chem. Soc.* **2023**, *145*, 6944−6952.
6 Wang, N. W.; Hong, R.; Zhang, G.; Pan, M. H.; Bao, Y. L.; Zhang, W. Molecular imprinting strategy enables circularly polarized luminescence enhancement of recyclable chiral polymer films. *Small* **2025**, *21*, 2409078.
7 Palaprat, G.; Mingotaud, A.; Langevin, D.; Mauzac, M.; Marty, J. Molecularly imprinted cholesteric materials for enhanced enantiomeric separation. *Polymer* **2022**, *243*, 124654.
8 Wu, G. Recent advances in helical polyacetylene derivatives used as coated chiral stationary phases for enantioseparation. *Polym. Chem.* **2022**, *13*, 3036−3047.
9 Ishiwari, F.; Takata, T. Cyclodextrin-based chiral rotaxane systems: design and functions. *Front. Chem.* **2022**, *10*, 1025977.
10 Qin, W. D.; Li, J. S.; Li, C. H.; Zeng, Q. H.; Teng, Q.; Yang, Y. Y.; Li, J.

Graphical Abstract

Generation and Modulation of Apparent All-angle Dependent Nonreciprocal Chiroptical Response in Chiral Polyurethane Film

Run Zhang, Biao Zhao, and Jian-Ping Deng

Beijing University of Chemical Technology

Chiral polyurethane (BPU) containing binaphthol (BINOL) groups in the main chain was prepared. By introducing specific small-molecule doping into this system, a significant non-reciprocal chiroptical response can be induced in the BPU. Through removal of excess doped small molecules and control experiments, this study successfully demonstrated that small-molecule doping is the core cause of the nonreciprocal chiroptical response in the BPU system.

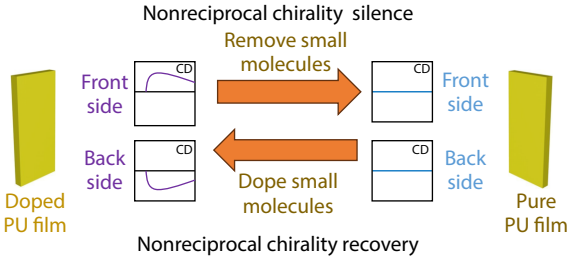

Chinese J. Polym. Sci. 2026 *https://doi.org/10.1007/s10118-026-3792-5*

Y.; Liao, K. L.; Hou, M. Y.; Tan, Q. H.; Xu, X.; Chen, Y. G.; Hu, Y. C.; Zeng, Z. W.; Zhang, X.; Yuan, F. L. Helical nanoconfinement in recyclable chiral soft photonic crystals enables strong and efficient full-color circularly polarized luminescence from carbon quantum dots. *Angew. Chem. Int. Ed.* **2026**, *65*, e4885590.

11 Li, J. S.; Qin, W. D.; Li, C. H.; Yang, Y. Y.; Liao, K. L.; Yuan, F. L. Efficient and high color-purity red and deep-red circularly polarized luminescence from carbon quantum dots enabled by helical co-assembly strategy. *Adv. Funct. Mater.* **2025**, *35*, 2510409.

12 Li, L. L.; Jiang, P. T.; Chen, L.; Li, Y.; Cheng, Y. X. Excitation-dependent circularly polarized luminescence triggered by selective excitation of achiral dichroic dyes in cholesterol liquid crystals. *Chem. Sci.* **2025**, *16*, 21583–21589.

13 Li, J. Y.; Liao, K. L.; Zeng, Q. H.; Zhang, X.; Zhang, J. J.; Yuan, F. L. Harnessing reversible 0d-1d transformation in chiral Mn(II) halides for smart circularly polarized luminescence switching and multi-level encryption. *Angew. Chem. Int. Ed.* **2026**, *65*, e25831.

14 Lian, Z.; Liu, L.; He, J.; Fan, S. M.; Guo, S. Z.; Li, X. A.; Liu, G. Q.; Fan, Y. Q.; Chen, X. B.; Li, M.; Chen, C. F.; Jiang, H. Structurally diverse pyrene-decorated planar chiral [2,2]paracyclophanes with tunable circularly polarized luminescence between monomer and excimer. *Chem. Eur. J.* **2024**, *30*, e202303819.

15 Guo, C. H.; Zhao, W. L.; Tan, K. K.; Guo, W. C.; Feng, L. H.; Chen, C. F.; Li, M. Axial enantiomers with donor-regulated TADF feature for multicolor circularly polarized electroluminescence. *Sci. China Chem.* **2024**, *67*, 2039–2045.

16 Wang, X.; Song, Q. P.; He, Z. X.; Zhang, G.; Miao, T. F.; Cheng, X. X.; Zhang, W. Constructing diverse switchable circularly polarized luminescence *via* a single azobenzene polymer film. *Chin. Chem. Lett.* **2025**, *36*, 110047.

17 Wang, Q.; Liu, Y. Q.; Wu, Z. Q. Synthesis and structure control of chiral helical polymers. *Chin. J. Org. Chem.* **2023**, *43*, 4141–4146.

18 Wang, S.; Sun, X. Q.; Zeng, H.; Xie, S. Y.; Zhang, J.; Wan, X. H. Postpolymerization modification-induced chiral self-assembly of substituted poly(phenylacetylene)s based on cis-transoid to cis-cisoid helical transition. *Macromolecules* **2025**, *58*, 1235–1244.

19 Zhang, G.; Bao, Y. L.; Ma, H. T.; Wang, N. W.; Cheng, X. X.; He, Z. X.; Wang, X.; Miao, T. F.; Zhang, W. Precise modulation of circularly polarized luminescence *via* polymer chiral co-assembly and contactless dynamic chiral communication. *Angew. Chem. Int. Ed.* **2024**, *63*, e202401077.

20 Gao, R. T.; Zong, Y.; Li, T. T.; Liu, N.; Wu, Z. Q. Three-dimensional supramolecular polymer frameworks with precisely tunable and large apertures for enzyme encapsulation. *Chin. Chem. Lett.* **2026**, *37*, 111582.

21 Liu, B. H.; Zong, Y.; Liu, N.; Wu, Z. Q. Advances in self-assembly-based circularly polarized luminescent materials. *Sci. China Chem.* **2024**, *67*, 3247–3257.

22 Albano, G.; Pescitelli, G.; Di Bari, L. Chiroptical properties of thin films of π-conjugated systems. *ChemNanoMat* **2022**, *8*, e202200219.

23 Yao, Y.; Ugras, T. J.; Meyer, T.; Dykes, M.; Wang, D.; Arbe, A.; Bals, S.; Kahr, B.; Robinson, R. D. Chiral 2D perovskites with a high degree of lead octahedral distortion and large circular dichroism. *ACS Nano* **2022**, *16*, 20457–20469.

24 Han, X.; Wang, W.; Jin, M.; Jing, C.; Liang, B.; Chai, C.; Xiong, R.; Zhang, W. Unveiling chiral perovskite cd signal scaling: discerning authentic and counterfeit signals through sample-state analysis. *Anal. Chem.* **2023**, *95*, 16201–16209.

25 Zinna, F.; Albano, G.; Taddeucci, A.; Colli, T.; Aronica, L. A.; Pescitelli, G.; Di Bari, L. Emergent nonreciprocal circularly polarized emission from an organic thin film. *Adv. Mater.* **2020**, *32*, 2002575.

26 Albano, G.; Salerno, F.; Portus, L.; Porizo, W.; Aronica, L. A.; Di Bari, L. Outstanding chiroptical features of thin films of chiral oligothiophenes. *ChemNanoMat* **2018**, *4*, 1059–1070.

27 Salij, A.; Goldsmith, R. H.; Tempelaar, R. Theory of apparent circular dichroism reveals the origin of inverted and noninverted chiroptical response under sample flipping. *J. Am. Chem. Soc.* **2021**, *143*, 21519–21531.

28 Parrish, K. A.; Salij, A.; Kamp, K. R.; Smith, E.; Utama, M. I. B.; Bergsten, A. J.; Czerwinski, R.; Smith, M. A.; Hersam, M. C.; Poeppelmeier, K. R.; Goldsmith, R. H.; Tempelaar, R. Differential absorption of circularly polarized light by a centrosymmetric crystal. *Science* **2025**, *388*, 1194–1197.

29 Xi, P.; Cao, Y.; Tan, T.; Ye, X.; Programmable chiroptical multilayer films assembled from self-healing stretchable elastomers for information encryption. *J. Mater. Chem. C* **2025**, *13*, 15398−15410.
30 Jin, L.; Mo, W.; Wang, Z.; Hong, W. Vortex-enabled nonreciprocal circularly polarized luminescence in achiral polymer systems. *Adv. Funct. Mater*. **2025**, e21524.
31 Huang, Y. H.; Kang, S. M.; Cai, S. L.; Zhang, Z. H.; Yu, P. Y.; Sun, X. Q.; Wan, X. H.; Zhang, J. Tunable mesoscale chirality in two-dimensional vortex-like assemblies of helically grooved poly(phenylacetylene) derivatives. *J. Am. Chem. Soc.* **2025**, *147*, 40849−40858.
32 Kang, S. M.; Chen, M. X.; Li, Y.; Sun, X. Q.; Liu, Y. Z.; Wang, S.; Zhang, J.; Wan, X. H. Mechanofluorochromic elastomers based on reversible helical transition of poly(phenylacetylene)s. *Angew. Chem. Int. Ed.* **2025**, *64*, e202513866.
33 Gao, R. T.; Kang, S. M.; Zong, Y.; Li, T. T.; Liu, N.; Wu, Z. Q. Polymer frameworks with controllable pore size and chirality for enantioseparation of racemates with different sizes and chiralities. *CCS Chem*. **2026**, doi: 10.31635/ccschem.026.202506825.
34 Gao, R. T.; Ma, Y. Y.; Xu, Y.; Wang, J.; Liu, N.; Liu, F.; Wu, Z. Q. Eugenol-based optically active helical polymers: from controlled synthesis to post-polymerization modification and chiral recognition. *Sci. China Mater.* **2026**, *69*, 2574−2582.
35 Gao, R. T.; Li, S. Y.; Liu, N.; Liu, B. H.; Wu, Z. Q. Helical polymers: from precise synthesis to structures and functions. *Chem. Rev.* **2026**, *126*, 297−403.
36 Li, P.; Zhao, B.; Pan, K.; Deng, J. Synergism between LDLB and true CD to achieve angle-dependent chiroptical inversion and switchable polarized luminescence emission in nonreciprocal nanofibrous films. *Nanoscale* **2023**, *15*, 5345−5364.
37 Li, P.; Deng, J. Switchable chiroptical flexible films based on chiral helical superstructure: handedness inversion and dissymmetric adjustability by stretching. *Adv. Funct. Mater.* **2021**, *31*, 2105315.
38 Zhang, R.; Song, L.; Yin, W.; Zhao, B.; Deng, J. Generation and modulation of nonreciprocal chirality to realize nonreciprocal CPL emission in polyurethane films. *Sci. China Chem.* **2025**, *68*, 3247−3259.
39 Deng, J.; Tabei, J.; Shiotsuki, M.; Sanda, F.; Masuda, T. Dynamically stable helices of poly(N-propargylamides) with bulky aliphatic groups. *Macromolecules* **2004**, *37*, 5149−5154.
40 Schrock, R. R.; Osborn, J. A. .pi.-Bonded complexes of the tetraphenylborate ion with rhodium(I) and iridium(I). *Inorg. Chem*. **1970**, *9*, 2339−2343.
41 Mirhosseini, M. M.;Haddadi-Asl, V.; Khordad, R. Molecular dynamics simulation, synthesis and characterization of polyurethane block polymers containing PTHF/PCL mixture as a soft segment. *Polym. Bull.* **2022**, *79*, 643−661.
42 Pan, R.; Wang L. L.; Shanks, R.; Liu, Y. The influence of trisilanolisobutyl poss on domain microstructure of a polyurethane hybrid composite: a molecular simulation approach. *Silicon* **2019**, *11*, 2253−2260.
43 Lu, J.; Wu, W.; Colombari, F. M.; Jawaid, A.; Seymour, B.; Whisnant, K.; Zhong, X.; Choi, W.; Lahann, J.; Vaia, R. A.; de Moura, A. F.; Nepal, D.; Kotov, N. A. Nano-achiral complex composites for extreme polarization optics. *Nature* **2024**, *630*, 860−868.